

## Characterization of Structural Stability of Magnetron Sputtered Tungsten-boron Thin Films at Elevated Temperatures

Liga AVOTINA<sup>1\*</sup>, Annija Elizabete GOLDMANE<sup>1</sup>, Edgars VANAGS<sup>2</sup>,  
Aija TRIMDALE-DEKSNE<sup>3</sup>, Lada BUMBURE<sup>4</sup>, Marina ROMANOVA<sup>4</sup>,  
Hermanis SOROKINS<sup>4</sup>, Alexei MUHIN<sup>5</sup>, Aleksandrs ZASLAVSKIS<sup>5</sup>, Gunta KIZANE<sup>1</sup>,  
Yuri DEKHTYAR<sup>4</sup>

<sup>1</sup> Institute of Chemical Physics, University of Latvia, Jelgavas str. 1, Riga, Latvia

<sup>2</sup> Institute of Solid State Physics, University of Latvia, Kengaraga str. 8, Riga, Latvia

<sup>3</sup> Faculty of Chemistry, University of Latvia, Jelgavas str. 1, Riga, Latvia

<sup>4</sup> Institute of Biomedical Engineering and Nanotechnologies, Riga Technical University, Kipsalas str. 6B, Riga, Latvia

<sup>5</sup> Joint-stock company "ALFA RPAR", Ropazu str. 140, Riga, Latvia

<http://doi.org/10.5755/j02.ms.32082>

Received 19 August 2022; accepted 17 November 2022

In the divertor of the tokamak type fusion reactors tungsten and tungsten-covered plasma facing materials are currently among the selected materials. However, metallic, high-Z plasma facing materials require plasma mitigation. Recent researches show, that mitigation with boron can be used for optimizing plasma operations, while the interactions between boron containing plasma and tungsten plasma facing materials are less investigated. The formation of mixed layers and their behaviour under plasma operations as well as reactor maintenance procedures needs to be estimated. In order to estimate properties of tungsten-boron mixed layers, such layers can be produced by deposition methods, such as the magnetron sputtering technique and further characterized and analysed. Magnetron sputtered tungsten-boron films were oxidized up to 600 °C. Prior and after thermal treatment infrared spectra and electron microscopy images of the films were registered. For comparison, W films with no addition B of were deposited. Selected parts of the films were etched, to analyse temperature dependent edge effects. Mass changes at ~ 400–500 °C can be attributed to the corresponding oxidation processes. The structure analysis and infrared spectrometry show the formation of W-O and W=O bonds. The obtained results will be applied for recommendations for the production of W-B thin films for microelectronic devices.

*Keywords:* tungsten, tungsten boride, thermal analysis, structural changes.

### 1. INTRODUCTION

Energy production in fusion reactors is promoted as a sustainable future energy source. Among the challenges for the optimal operation and maintenance of the fusion reactors is the selection of plasma facing materials and their behavior during plasma reactions. Tungsten-boron compounds ( $W_xB_y$ ) belong to the group of superhard materials [1] and have a wide application in microelectronic devices [2], as coating material in harsh conditions [3], they are promising in application for gamma radiation shielding [4], in photovoltaic cells, as well as for field emission vacuum solid triodes [5], as well as for superconductors in the fusion devices [6].

The formation of  $W_xB_y$  compounds takes place during plasma operations of the fusion devices, where boron is used to mitigate plasma [7]. The mitigation process together with plasma reactions causes several processes such as formation of deposited layers [8, 9], changes in surface chemical composition and structure [10], aging of divertor materials [11], affecting the lifetime of construction parts [12], and changing the properties of plasma facing surfaces [13]. Moreover, the deposition and formation of co-deposited layers is among the main processes leading to the retention

and accumulation of fusion fuel atoms – deuterium and tritium [14].

To explore the effects that take place in the vacuum vessel of the fusion reactor, related to the deposited layers, a magnetron sputtering technique [15–17] is widely used. Although thermal analysis of the deposited films allows exploration of the behaviour of the deposits under maintenance procedures, such as vacuum vessel baking [18], as well as expand the knowledge about processes under loss of vacuum, that is needed to ensure fault free operations.

This work is focused on thermal behaviour of magnetron sputtered  $W_xB_y$  thin films and comparison with W films without boron additions.

### 2. EXPERIMENTAL

The  $W_xB_y$  films were deposited on the Si/SiO<sub>2</sub> substrate by the direct current magnetron sputtering technique, in argon, using a WB<sub>2</sub> target. For comparison, W (W target) films with no addition of B were deposited. Deposition time was 20 min at 150 °C. The thickness of the films was determined by applying a Mitutoyo surface roughness tester and estimated to be 150 nm. Selected parts of the films were

\* Corresponding author. Tel.: +371 67033937; fax: +371 67033937.  
E-mail: [liga.avotina@lu.lv](mailto:liga.avotina@lu.lv) (L. Avotina)

etched by applying chemical treatment (Alfa RPAR Ltd.). An example of the scheme of the fabricated coating and a photograph of the coated sample are shown in Fig. 1.

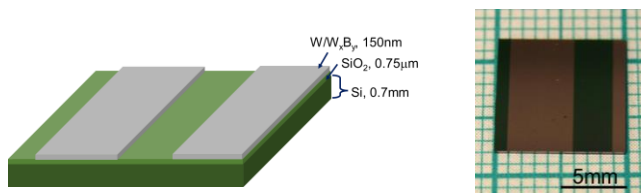


**Fig. 1.** Scheme of the fabricated  $W_xB_y$  coating and a photograph of the coated sample

Thermal treatment was performed in air to facilitate the aging processes and examine the impact of the presence of oxygen in the vacuum vessel. The coatings were oxidized with a temperature regime of  $10\text{ }^\circ\text{C}/\text{min}$ , up to  $600\text{ }^\circ\text{C}$  and an exposure time of 1 h, followed by cooling down to room temperature in a Nabetherm muffle furnace. For thermal analysis in the SEIKO EXSTAR 6300 device, the fabricated samples were cut in the pieces with a diameter of 5 mm to fit in the  $Al_2O_3$  crucibles. Thermal analysis was performed with the same temperature parameters as for the muffle furnace. Thermogravimetry (TG, mass measurements), differential thermal analysis (DTA, exothermic and endothermic effects) and differential thermal analysis (DTG, mass change rate) measurements registered during heating. Prior and after thermal treatment infrared spectra of the films were recorded with Bruker Vertex 70v Fourier Transform Infrared (FTIR) spectrometer, vacuum 2.95 hPa, attenuated total reflection mode, range  $400\text{--}4000\text{ cm}^{-1}$ , resolution  $\pm 2\text{ cm}^{-1}$ , at least 3 measurements per sample were made, 20 spectra per measurement recorded.

For scanning electron microscopy (SEM) analysis, samples were adhered to Al stubs using conductive carbon adhesive tape. Morphology and element content in deposited films were evaluated by a high-resolution field emission SEM apparatus Thermo Scientific™ Helios™ 5 UX (University of Latvia, Institute of Solid State Physics). The working distance was set to 4 mm. The SEM images were collected at a 2 kV electron acceleration voltage, a 25 pA current by detecting secondary electrons using a through-the-lens detector, ion conversion and electron detector, while energy-dispersive X-ray spectroscopy (EDS) was performed at an acceleration voltage of 15 kV.

### 3. RESULTS AND DISCUSSION

Two types of deposited layers were compared. The SEM analysis was applied for surface structure characterization, while element content was estimated with EDS analysis, while the chemical bonds were examined with FTIR. In the thermal analysis the differences between DTA, TG and DTG curves of both types of films were examined.

#### 3.1. Surface morphology

An EDS spectrum of a  $W_xB_y$  film is shown in Fig. 2. The Si and O signals occur due to the electron beam penetration through the layer. The boron as a light element is hardly distinguishable in the EDS spectrum. However, the quantification option allows us to determine the

approximate stoichiometry of  $W_xB_y$  to be  $WB_2$ .

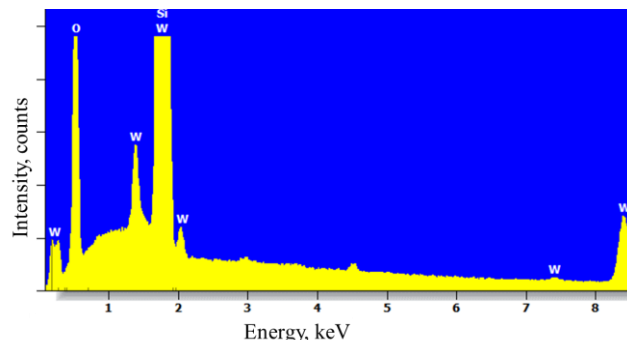


**Fig. 2.** EDS spectrum of boron containing W thin film on Si-SiO<sub>2</sub> substrate

SEM analysis shows formation of homogeneously rough surface, while addition of boron results in comparably smoother surface (Fig. 3, upper images).

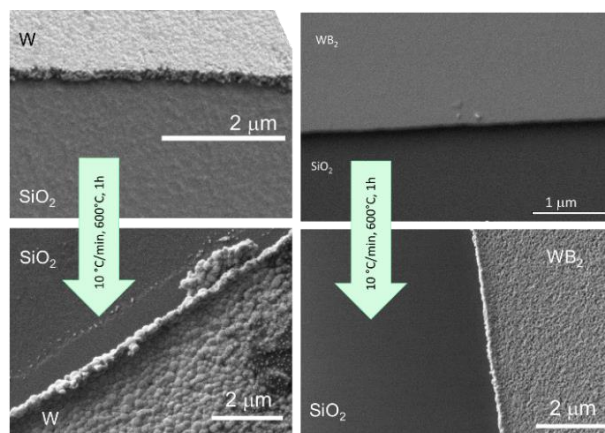


**Fig. 3.** Thermally induced surface modifications in W and  $WB_2$  coatings

Thermally treated films both have a homogeneous rough surface. Additionally, it is observed that the edges of thermally treated films tend to detach from the substrate (Fig. 3, bottom images). This effect shows, that films deposited in the vacuum vessel of the fusion reactor, in the presence of oxygen, which can be possible during maintenance procedures or loss of vacuum cases, can detach from the surfaces and subsequently result in a form of dust.

#### 3.2. Analysis of chemical bonds

Analysis of chemical bonds show that in the W coating no signals occur, while in spectra of  $WB_2$  some weak signals occur, which are assigned to Si-O bonds from the substrate.

In the FTIR spectra of W films no signals occur, showing that no signal from the  $SiO_2$  substrate penetrates through the film. In the FTIR spectra of the Si-SiO<sub>2</sub>- $WB_2$  films the peaks around 455, 515, 840 and  $1100\text{ cm}^{-1}$  (Fig. 4) correspond to the Si-O [19] from the  $SiO_2$ , leading to an increased IR photon permeability through the film and less dense deposition mechanism as for pure tungsten. Peaks at 595, 675, 800 correspond to W-O and W=O bonds, while peaks at 1010, 1050,  $1100\text{ cm}^{-1}$  are related to Si-O bonds [19]. In the spectra of the oxidized  $WB_2$  films peak at 640 is related to W-O bonds, while the peak at  $935\text{ cm}^{-1}$  could correspond to the B-O bond [20]. The presence of Si-O

bonds shows restructuring of the film leading to a lower density, IR photon permeability as well as possible formation of pores, which can serve as deposition points for fuel atoms in a fusion reactor.

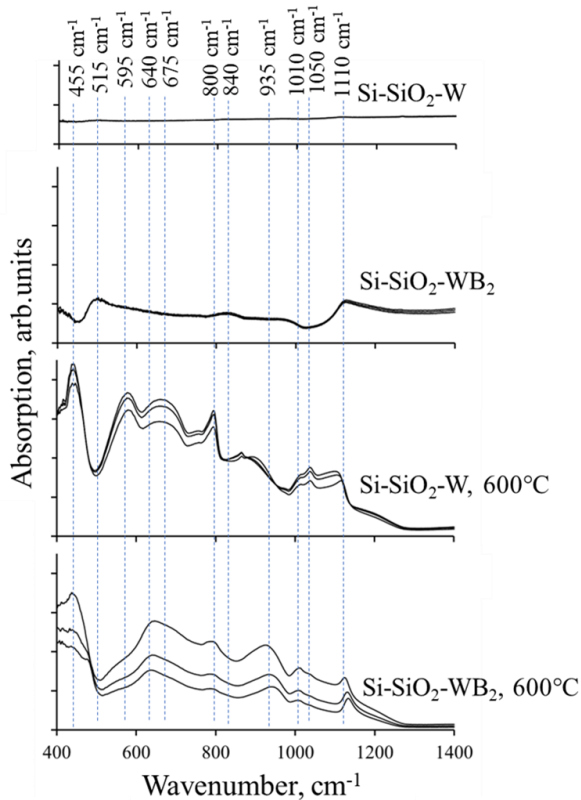


**Fig. 4.** FTIR spectra of nontreated and thermally treated W and WB<sub>2</sub> coatings

### 3.3. Thermal processes

The TG and DTG curves of W and WB<sub>2</sub> films show to an increase in mass. The TG/DTA/DTG curves of WB<sub>2</sub> film are presented in Fig. 5. Mass changes are correlating with oxygen attraction to the surface and reaction with boron [21] and tungsten [22, 23] atoms. A mass increase for both coatings is similar and continues at high temperature exposure and the cooling process.

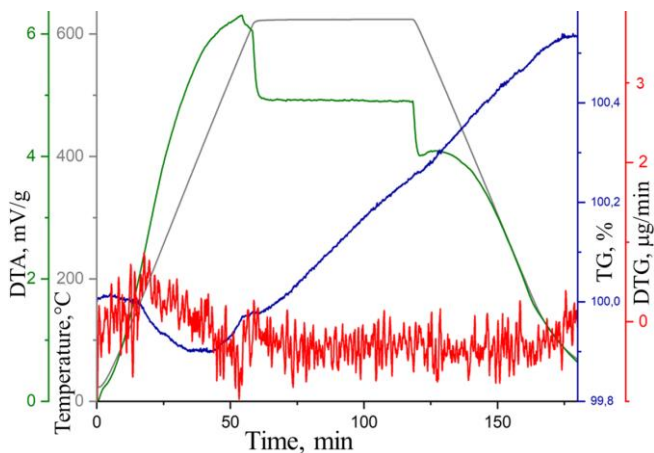


**Fig. 5.** TG/DTA/DTG curves of 150nm WB<sub>2</sub> film

When comparing the processes of mass change, no significant differences were observed between W and WB<sub>2</sub>,

while the DTA curves show to slightly increased slope of the exothermic reaction for the W and an endothermic signal for WB<sub>2</sub> around 580 °C (indicated in Fig. 6), corresponding to the thermal stability edge of the WB<sub>2</sub> powder [24].

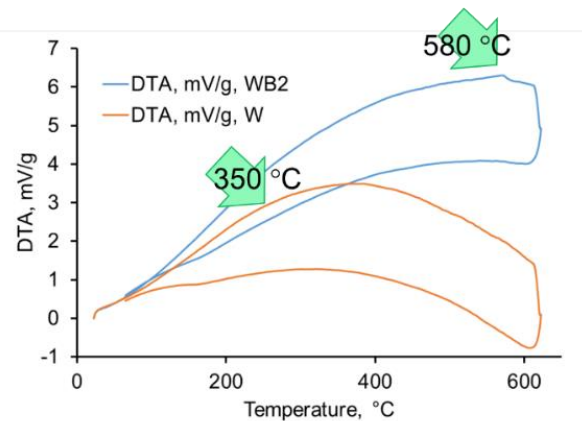


**Fig. 6.** DTA curves of W and WB<sub>2</sub> during the thermal treatment process

Differences in the thermal behaviour should be considered for the development of the maintenance procedures for the fusion reactors, where tungsten is proposed as plasma facing material and boron as mitigating element.

## 4. CONCLUSIONS

The magnetron sputtering technique applied as a tool for developing layers for investigation of the plasma-wall interaction processes of the fusion reactors gives impact on understanding layers modification processes in the presence of oxygen.

The application of thermal treatment of synthesized layers simulates aging processes and allows us to compare layers with different composition.

The Addition of the B to W layers changes the thermal behaviour under presence of oxygen. This should be taken into for modelling of the aging materials and for evaluation of the processes that take place during impurity seeding.

### Acknowledgments

The research is supported by the ERDF project No. 1.1.1.1/20/A/109 «Planar field emission microtriode structure». Institute of Solid State Physics, University of Latvia as the Center of Excellence has received funding from the European Union's Horizon 2020 Framework Programme H2020-WIDESPREAD-01-2016-2017-TeamingPhase2 under grant agreement No.739508, project CAMART2.

### REFERENCES

1. Chrzanowska-Giżyńska, J., Denis, P., Woźniacka, S., Kurpaska, L. Mechanical Properties and Thermal Stability of Tungsten Boride Films Deposited by Radio Frequency Magnetron Sputtering *Ceramics International* 44 (16) 2018: pp. 19603–19611. <https://doi.org/10.1016/j.ceramint.2018.07.208>

2. **Moraes, V., Riedl, H., Fuger, Chr., Polcik, P., Bolvardi, H., Holec, D., Mayrhofer, P.H.** Ab Initio Inspired Design of Ternary Boride Thin Films *Scientific Reports* 8 2018: pp. 9288.  
<https://doi.org/10.1038/s41598-018-27426-w>
3. **Sun, Sh., Wang, H., Liu, X., Liu, Ch., Lu, H., Nie, Z., Song, X.** Outstanding Anti-Oxidation Performance of Boride Coating Under High-Temperature Friction *Corrosion Science* 179 2021: pp. 109133.  
<https://doi.org/10.1016/j.corsci.2020.109133>
4. **Windsor, C.G., Astbury, J.O., Davidson, J.J., McFadzean, Ch.J.R., Morgan, J.G., Wilson, Chr.L., Humphry-Bake, S.A.** Tungsten Boride Shields in a Spherical Tokamak Fusion Power Plant *Nuclear Fusion* 61 (086018) 2021: pp. 1–14.  
<https://doi.org/10.1088/1741-4326/ac09ce>
5. **Koshevaya, S.V., Kanevsky, V.I., Tecpoyotl-T, M., Gutiérrez-D, E.A., Burlak, G.N., Chayka, V.E.** Vacuum-Silicon Solid Microwave Diodes and Triodes Based on P++-N and on Tungsten Cathodes *Microelectronics Journal* 32 (2) 2001: pp. 173–175.  
[https://doi.org/10.1016/S0026-2692\(00\)00111-7](https://doi.org/10.1016/S0026-2692(00)00111-7)
6. **Kayhan, M., Hildebrandt, E., Frotscher, M., Senyshyn, A., Hofmann, K., Alff, L., Albert, B.** Neutron Diffraction and Observation of Superconductivity for Tungsten Borides, WB and W<sub>2</sub>B<sub>4</sub> *Solid State Sciences* 14 (11–12) 2012: pp. 1656–1659.  
<https://doi.org/10.1016/j.solidstatesciences.2012.05.036>
7. **Gilson, E.P., Lee, H.H., Bortolon, A., Choe, W., Diallo, A., Hong, S.H., Lee, H.M., Lee, J., Maingi, R., Mansfield, D.K., Nagy, A., Park, S.H., Song, I.W., Song, J.I., Yun, S.W., Yoon, S.W., Nazikian, R.** Wall Conditioning and ELM Mitigation with Boron Nitride Powder Injection in KSTAR *Nuclear Materials and Energy* 28 2021: pp. 101043.  
<https://doi.org/10.1016/j.nme.2021.101043>
8. **Sun, L., Wu, D., Li, C., Wu, J., Hong, S.H., Bang, E., Hu, Z., Ding, F., Luo, G., Ding, H.** Characterization of the Impurity Features Deposited on the Boronization Tungsten Tiles Exposed in KSTAR Tokamak Using Laser-Induced Breakdown Spectroscopy *Nuclear Materials and Energy* 31 (101174) 2022: pp. 1–8.  
<https://doi.org/10.1016/j.nme.2022.101174>
9. **Baron-Wiechec, A., Widdowson, A., Alves, E., Ayres, C.F., Barradas, N.P., Brezinsek, S., Coad, J.P., Catarino, N., Heinola, K., Likonen, J., Matthews, G.F., Mayer, M., Petersson, P., Rubel, M., van Renterghem, W., Uytendhouwen, I.** Global Erosion and Deposition Patterns in JET With the ITER-Like Wall *Journal of Nuclear Materials* 463 2015: pp. 157–161.  
<https://doi.org/10.1016/j.jnucmat.2015.01.038>
10. **Fan, C., Liu, C., Peng, F., Tan, N., Tang, M., Zhang, Q., Wang, Q., Li, F., Wang, J., Chen, Y., Liang, H., Guan, S., Yang, K., Liu, J.** Phase Stability and Incompressibility of Tungsten Boride (WB) Researched by In-Situ High Pressure X-Ray Diffraction *Physica B: Condensed Matter* 512 2017: pp. 6–12.  
<https://doi.org/10.1016/j.physb.2017.06.028>
11. **Imran, M., Hai, R., Sun, L.Y., Sattar, H., He, Z.L., Wu, D., Li, C., Wang, W.J., Hu, Z.H., Luo, G.N., Ding, H.** Characterization of Multi-Element Impurity Deposited on EAST Divertor Tile Using Laser-Induced Breakdown Spectroscopy *Journal of Nuclear Materials* 526 (151775) 2019: pp. 1–12.  
<https://doi.org/10.1016/j.jnucmat.2019.151775>
12. **Hanada, K., Yoshida, N., Hasegawa, M., Oya, M., Oya, Y., Takagi, I., Hatayama, A., Shikama, T., Idei, H., Nagashima, Y., Ikezoe, R., Onchi, T., Kuroda, K., Kawasaki, S., Higashijima, A., Nagata, T., Shimabukuro, S., Nakamura, K., Murakami, S., Takase, Y., Gao, X., Liu, H., Qian, J.** Overview of Recent Progress on Steady State Operation of All-Metal Plasma Facing Wall Device QUEST *Nuclear Materials and Energy* 27 (101013) 2021: pp. 1–8.  
<https://doi.org/10.1016/j.nme.2021.101013>
13. **Miyamoto, M., Tokunaga, K., Fujiwara, T., Yoshida, N., Morimoto, Y., Sugiyama, T., Okuno, K.** Material Properties of Co-Deposition Formed on Plasma Facing Materials in All-Metal Machine TRIAM-1M *Journal of Nuclear Materials* 313–316 2003: pp. 82–86.  
[https://doi.org/10.1016/S0022-3115\(02\)01352-1](https://doi.org/10.1016/S0022-3115(02)01352-1)
14. **Dittrich, L., Petersson, P., Rubel, M., Thien Tran, T., Widdowson, A., Jezu, I., Porosnicu, C., Alves, E., Catarino, N.** JET Contributors Fuel Retention and Erosion-Deposition on Inner Wall Cladding Tiles in JET-ILW *Physica Scripta* 96 (124071) 2021: pp. 1–13.  
<https://doi.org/10.1088/1402-4896/ac379e>
15. **Kelly, P.J., Arnell, R.D.** Magnetron Sputtering: a Review of Recent Developments and Applications *Vacuum* 56 (3) 2000: pp. 159–172.  
[https://doi.org/10.1016/S0042-207X\(99\)00189-X](https://doi.org/10.1016/S0042-207X(99)00189-X)
16. **Yang, J., Yang, Z., Lei, X., Huang, J., Chen, S., Ye, Z., Zhao, Y.** Behavior and Mechanism for Boron Atom Diffusing Across Tungsten Grain Boundary in the Preparation of WB Coating: A First-Principles Calculation *Applied Surface Science* 543 2021: pp. 1–12.  
<https://doi.org/10.1016/j.apsusc.2020.148778>
17. **Soni, K., Moser, L., Porosnicu, C., Antunes, R., Arredondo, R., Dinca, P., Steiner, R., Marot, L., Meyer, E.** Deuterium Plasma Sputtering of Mixed Be-W Layers *Journal of Nuclear Materials* 564 (153671) 2022: pp. 1–8.  
<https://doi.org/10.1016/j.jnucmat.2022.153671>
18. **Likonen, J., Heinola, K., De Backer, A., Baron-Wiechec, A., Catarino, N., Jezu, I., Ayres, C.F., Coad, P., Koivuranta, S., Krat, S., Matthews, G.F., Mayer, M., Widdowson, A.** Investigation of Deuterium Trapping and Release in the JET ITER-Like Wall Divertor Using TDS and TMAP *Nuclear Materials and Energy* 19 2019: pp. 166–178.  
<https://doi.org/10.1016/j.nme.2019.02.031>
19. **Goldmane, A.E., Avotina, L., Romanova, M., Muhin, A., Zaslavskis, A., Kizane, G., Dekhtyar, Y.** FTIR Analysis of Oxidized Tungsten and Tungsten Diboride Nanolayers *Materials Science (Medžiagotyra)* 28 (3) 2022: pp. 1–4.  
<https://doi.org/10.5755/j02.ms.29796>
20. **Peak, D., Luther, G.W., Sparks, D.L.** ATR-FTIR Spectroscopic Studies of Boric Acid Adsorption on Hydrous Ferric Oxide *Geochimica et Cosmochimica Acta* 67 (14) 2003: pp. 2551–2560.  
[https://doi.org/10.1016/S0016-7037\(03\)00096-6](https://doi.org/10.1016/S0016-7037(03)00096-6)
21. **Wang, J., Zhu, B., Sun, Y.** Microscopic Mechanism of  $\alpha$ -Rhombic Crystal Boron Nanocluster Oxidation in Oxygen *Fuel* 31 C 122448 2022: pp. 1–11.  
<https://doi.org/10.1016/j.fuel.2021.122448>
22. **Warren, A., Nylund, A., Olefjord, I.** Oxidation of Tungsten and Tungsten Carbide in Dry and Humid Atmospheres *International Journal of Refractory Metals and Hard Materials* 14 (5–6) 1996: pp. 345–353.  
[https://doi.org/10.1016/S0263-4368\(96\)00027-3](https://doi.org/10.1016/S0263-4368(96)00027-3)

23. **Pandurangarao, K., Ravi Kumar, V.** Preparation and Characterization of Nanocrystalline Tungsten Oxide Thin Films for Electrochromic Devices: Effect of Deposition Parameters *Materials Today: Proceedings* 19 (16) 2019: pp. 2596–2603.  
<https://doi.org/10.1016/j.matpr.2019.10.093>
24. **Pangilinan, L.E., Turner, C.L., Akopov, G., Anderson, M., Mohammadi, R., Kaner, R.B.** Superhard Tungsten Diboride-Based Solid Solutions *Inorganic Chemistry* 57 2018: pp. 15305–15313.  
<https://doi.org/10.1021/acs.inorgchem>



Avotina © et al. 2023 Open Access This article is distributed under the terms of the Creative Commons Attribution 4.0 International License (<http://creativecommons.org/licenses/by/4.0/>), which permits unrestricted use, distribution, and reproduction in any medium, provided you give appropriate credit to the original author(s) and the source, provide a link to the Creative Commons license, and indicate if changes were made.